

Cancer-associated Fibroblast-derived IL-6 Promotes Head and Neck Cancer Progression via the Osteopontin-NF-kappa B Signaling Pathway.

Xing Qin^a, Ming Yan^a, Xu Wang^a, Qin Xu^{a, b}, Xiaoning Wang^a, Xueqin Zhu^a, Jianbo Shi^a, Zhihui Li^a, Jianjun Zhang^{a, #}, Wantao Chen^{a, b, #}

Affiliation of the authors:

^a Department of Oral and Maxillofacial-Head & Neck Oncology, Ninth People's Hospital, Shanghai Jiao Tong University School of Medicine, Shanghai, 200011, PR China.

^b Shanghai Key Laboratory of Stomatology & Shanghai Research Institute of Stomatology; National Clinical Research Center of Stomatology, Shanghai, 200011, PR China.

Corresponding Authors:

Wantao Chen, Ninth People's Hospital, Shanghai Jiao Tong University School of Medicine, 639 Zhizaoju Road, Shanghai 200011, China; Telephone: (86) 21-23271699-5210; Fax: (86) 21-63135412; E-mail: chenwantao196323@sjtu.edu.cn.

Jianjun Zhang, Ninth People's Hospital, Shanghai Jiao Tong University School of Medicine, 639 Zhizaoju Road, Shanghai 200011, China; Telephone: (86) 21-23271699-6509; E-mail: zjjshuobo@163.com.

Supplementary materials

Supplementary Materials and methods

Patients and specimens

All the samples, include tissues and plasma, were collected from the Department of Oral and Maxillofacial-Head and Neck Oncology, Ninth People's Hospital, Shanghai Jiao Tong University School of Medicine (Shanghai, China). More specifically, 60 pairs of tumor and adjacent normal tissues were obtained from the patients who were diagnosed with primary HNC and underwent initial surgery between June 2012 and December 2014. Half of each sample was quickly frozen in liquid nitrogen until the extraction of total RNA and protein, and the other half was embedded in paraffin for pathologic examination and immunohistochemical staining. In parallel, a separate cohort of 110 patients was assembled from a large pool of patients in the database based on histological diagnosis of HNC between April 2003 and April 2007. We retrospectively reviewed the medical records and follow-up data of these patients. The median follow-up time was 69.2 months and total RNAs of the 110 cases were extracted from paraffin blocks. Meanwhile, 96 specimens of normal oral epithelium taken from patients without HNC were used as the controls. Between September 2015 and December 2016, we recruited 137 patients with primary HNC, collected their plasma samples before surgery and stored at -80°C until further processing. In addition, plasma samples from 140 donors of physical examination in Ninth People's Hospital were selected as control group. In this study, written informed consent was

obtained from all participants involved in the study and the work was approved by the Medical Ethics Committee of the Ninth People's Hospital, Shanghai Jiao Tong University School of Medicine. None of these HNC patients received any preoperative cancer treatment and were histologically diagnosed as HNC after operation. Additionally, pathological differentiation and clinical stage were respectively determined according to World Health Organization Classification of Tumors and the TNM classification system of the International Union Against cancer (1988).

DNA extraction and sequencing

CAFs (HNC tissue derived) were sequenced at the KRAS exon 2 locus. Cells were washed, lysed with lysis buffer containing 25mM NaOH, 0.2mM EDTA, and boiled at 95°C for 30 min. Lysate was treated with 40mM Tris-HCl, 1.8mM EDTA, vortexed, and spun at 14,000 RPM for 15 min. PCR was performed with extracted DNA (forward primer: 5'-GGCCTGCTGAAAATGACTGA-3'; reverse primer: 5'-GTCCTGCACCAGTAATATGC-3') by using PrimeSTAR HS DNA Polymerase (Takara, Japan), and run on a 3% agarose gel via electrophoresis. DNA was spliced from gel and DNA extracted from gel with GeneElute™ Gel Extraction Kit (Sigma, USA). Samples were distributed to Sangon Biotech (Shanghai, China) for sequencing.

Primary antibodies

The antibodies used in this study were as follows: OPN rabbit polyclonal antibody

(Proteintech, USA); IL-6 rabbit polyclonal antibody (Proteintech, USA); Vimentin (V9) mouse monoclonal antibody (Sigma, USA); α -SMA (1A4) mouse monoclonal antibody (Abcam, USA); I κ B α (L35A5) mouse monoclonal antibody (CST, USA); p-I κ B α (Ser32/36) (5A5) mouse monoclonal antibody (CST, USA); NF- κ B p65 (L8F6) mouse monoclonal antibody (CST, USA), p-p65 (Ser468) mouse monoclonal antibody (CST, USA); p-p65 (Ser536) mouse monoclonal antibody (CST, USA); GAPDH (AG0766) mouse monoclonal antibody (Proteintech, USA); H3 histone rabbit polyclonal antibody (Beyotime, China); integrin β 1 (Y783) rabbit polyclonal antibody (Bioword, USA); integrin β 3 (S778) rabbit polyclonal antibody (Bioword, USA); integrin β 5 (V746) rabbit polyclonal antibody (Bioword, USA); integrin α (P804) rabbit polyclonal antibody (Bioword, USA); CD44 (E702) rabbit polyclonal antibody (Bioword, USA); STAT3 rabbit polyclonal antibody (Proteintech, USA); p-STAT3 (Tyr705) (D3A7) rabbit monoclonal antibody (CST, USA); OCT1 rabbit polyclonal antibody (Proteintech, USA); ETS-1 (D8O8A) rabbit monoclonal antibody (CST, USA); c-Jun (60A8) Rabbit monoclonal antibody (CST, USA); c-Myc (D3N8F) rabbit monoclonal antibody (CST, USA); Ki-67 (20Raj1) mouse monoclonal antibody (eBioscience, USA), MMP2 rabbit polyclonal antibody (Proteintech, USA), MMP9 rabbit polyclonal antibody (Proteintech, USA), uPA rabbit polyclonal antibody (Proteintech, USA) and ICAM-1 rabbit polyclonal antibody (Proteintech, USA).

Immunohistochemical analysis

Briefly, paraffin-embedded 3 μ m thick sections were deparaffinized, rehydrated,

submerged into citric acid buffer for heat-induced antigen retrieval, immersed in 0.3% hydrogen peroxide to block endogenous peroxidase activity, blocked with 3% bovine serum albumin, incubated with primary antibodies at 4°C overnight and developed using the DAKO ChemMate Envision Kit/HRP (Dako-Cytomation, USA). The sections were then counterstained with hematoxylin, dehydrated, cleared and mounted. The tissues exhibiting brown staining in the cytoplasm, nucleus or membrane were considered positive. Five targeted areas of each section were randomly selected under the same conditions for further analysis. The integrated optical density (IOD) of protein expression was quantitatively determined using Image-Pro Plus 6.0 software and calculated with the following formula: $MOD = IOD\ SUM / area\ SUM$ (MOD: mean optical density; IOD SUM: the accumulative IOD of targeted areas in one photo; area SUM: the sum of targeted areas). Primary antibodies were used at the following dilutions: OPN antibody (Proteintech, USA; 1:200), IL-6 antibody (Proteintech, USA; 1:200), NF- κ B p65 (L8F6) antibody (CST, USA; 1:400), Ki-67 (20Raj1) antibody (eBioscience, USA; 1:200), MMP2 antibody (Proteintech, USA; 1:200), MMP9 antibody (Proteintech, USA; 1:100), uPA antibody (Proteintech, USA; 1:200) and ICAM-1 antibody (Proteintech, USA; 1:200).

Western blot analysis

Cells were harvested at the indicated times and rinsed twice with PBS. Cell extracts were prepared with SDS lysis buffer (Beyotime, China) and centrifuged at $14,000 \times g$ for 10 min at 4°C. In addition, the NE-PER™ Nuclear and Cytoplasmic Extraction

Reagents (Thermo Fisher, USA) were used for separation and preparation of cytoplasmic and nuclear extracts from cultured cells. Protein samples (40 µg) were electrophoresed using 10% or 15% polyacrylamide gels and transferred to 0.45 µm PVDF membranes (Merck Millipore, USA). After the membranes were blocked with 5 % BSA for 1 h at room temperature, the blots were probed with OPN antibody (Proteintech, USA; 1:1,000), Vimentin (V9) antibody (Sigma, USA; 1:1,000), α-SMA (1A4) antibody (Abcam, USA; 1:300), STAT3 antibody (Proteintech, USA; 1:1,000); p-STAT3 (Tyr705) (D3A7) antibody (CST, USA; 1:1,000); IL-6 antibody (Proteintech, USA; 1:1,000), IκBα (L35A5) antibody (CST, USA; 1:1,000), p-IκBα (Ser32/36) (5A5) antibody (CST, USA; 1:1,000), NF-κB p65 (L8F6) antibody (CST, USA; 1:1,000), p-p65 (Ser468) antibody (CST, USA; 1:1,000) and p-p65 (Ser536) antibody (CST, USA; 1:1,000). GAPDH (AG0766) antibody (Proteintech, USA; 1:10,000) and H3 histone antibody (Beyotime, China; 1:2,000) were used throughout as loading controls. Secondary antibodies (Sigma, USA; 1:10,000) were labeled with IR Dyes. Signals were observed using an Odyssey Infrared Imaging System (Biosciences, USA).

ELISA analysis

Culture media of 1×10^6 cells were collected separately after incubation for 72 h and then centrifuged at $10,000 \times g$ for 10 min at 4°C. The supernatant OPN and IL-6 concentrations and the plasma OPN and IL-6 levels in patients with HNC were assessed using the Human OPN ELISA kit (Boster, China) and human IL-6 ELISA kit

(Boster, China). Moreover, the mouse OPN ELISA kit (Boster, China) was used to measure the plasma OPN level of nude mice. Briefly, 100 μ L standard samples and supernatant (both the culture media and plasma were diluted 10 times at first) were added into each microtiter plate well in triplicate and incubated for 90 min at 37 °C. Then, the liquid in each well was removed and 100 μ L biotin-labeled antibody dilution was added into each well directly. After incubation for 60 min at 37 °C, the wells were washed and 100 μ L avidin-peroxidase complex (ABC) dilution was added into each well. Thirty minutes later, the wells were washed and colored by incubation with tetramethyl benzidine (TMB) solution at 37 °C. Whereafter, the reactions were stopped and the absorbance (A)_{450 nm} values were measured by a microplate reader (Biohit, Helsinki, Finland) immediately. The standard curve was plotted using the concentration of the standard samples as the horizontal axis and the absorbance (A)_{450 nm} value as the vertical axis. The OPN and IL-6 concentration in culture media or plasma were calculated according to the formula of the standard curve.

Plasmid construction

The full-length sequences of OPN gene were amplified using PCR methods by a set of primers (forward primer: 5'-CGCAAATGGGCGGTAGGCGTG-3', reverse primer: 5'-CAGCGGGGCTGCTAAAGCGCATGC-3'). The amplified product of the OPN gene was purified, digested and ligated into the respective BanHI and EcoRI sites in the H102 vector (Obio Technology, China). Two individual constructs containing shRNA for human IL-6 and a negative control (i.e., a scrambled sequence) were

purchased from Obio Technology. The sequences were as follows: shIL-6-1, 5'-AGATAGAGCTTCTCTTTTCG-3'; shIL-6-2, 5'-CTCAGATTGTTGTTGTAA-3' and negative control, 5'-TTCTCCGAACGTGTCACGT-3'. The constructs were packaged for viral production as described below.

Lentivirus package and construction of OPN-expressing cell line

The 293T cells were cultured in DMEM medium supplemented with 5% FBS and transfected with 3 µg pLenti-OPN or pLenti-shRNA, 1 µg pCMV-VSV-G, and 3 µg pCMV-Delta8.9 using Lipofectamine 2000 reagent (Invitrogen, USA). After the cells were incubated overnight, the medium was replaced with 10 mL fresh medium. The virus-containing supernatants were collected at 48 and 72 h after transfection and then filtered using a 0.45 µm cellulose acetate filter (Merck Millipore, USA). The virus-containing supernatants were diluted 3 times with serum-free DMEM and polybrene (YEASEN, China) was added into the supernatants at the final concentration of 10 µg/mL to improve the efficiency of infection. The culture medium of tumor cells (at the density of 40%) was exchanged with the virus-containing mixture. After 8 h, the medium was exchanged with fresh DMEM culture medium. The OPN-expressing cells were selected with 10 µg/mL puromycin (Sigma, USA) for 3 weeks before experiments.

Transfection of small interfering RNAs

To knock down the expression of OPN and STAT3 in tumor cells, two OPN

gene-specific short interfering RNAs (siOPN-1 5'-GUGGGAAGGACAGUUAUGAdTdT-3' and siOPN-2 5'-CCACAGUAGACACAUAUGAdTdT-3') and three STAT3 gene-specific short interfering RNAs (siSTAT3-1 5'-AAAUGAAGGUGGUGGAGAAAdTdT-3', siSTAT3-2 5'-CAUCUGCCUAGAUCGGCUAdTdT-3' and siSTAT3-3 5'-CCCGUCAACAAAUUAAGAAAdTdT-3') were used. For transient transfection, tumor cells at 30% confluence were transfected with siRNAs using LipofectamineTM2000 reagent (Invitrogen, USA). The efficiency of OPN and STAT3 knock down was confirmed by Western blot analysis and qPCR after 48 h.

Plate colony formation assay

About 500 plasmid or siRNA-transfected tumor cells were cultured with DMEM supplemented with 10% FBS in 6-well plate for two weeks. Colonies were fixed with 4% paraformaldehyde and stained with crystal violet. The colony formation ability was evaluated according to the size and density of the colonies.

Soft agar colony formation assay

Twenty-four hours after tumor cells transfected with siRNA or plasmid, 3×10^3 cells were mixed with 1 mL of 0.5% agarose in DMEM with 10% FBS, then seeded on the top of solidified 1% agarose in 6-well plate in triplicates. The gel was covered with 500 μ L of DMEM medium after the top layer was solidified, added 100 μ L DMEM medium every week to prevent the gel drying. The gels incubated for 3-4 weeks until the colonies formed obviously, then colonies > 0.1 mm in diameter were counter

under a microscopic field at 20× magnification. 3 independent experiments were finished in this study.

Transwell migration and invasion assay

The cell migration assay was performed with transwell chamber (pores 0.8 μm, Merck Millipore, USA), while the cell invasion assay was implemented with Matrigel (BD Biosciences, USA) coated on the upper surface of the transwell chamber (pores 0.8 μm, Merck Millipore, USA). Briefly, tumor cells (3×10^4 cells for migration assay and 5×10^4 cells for invasion assay) in 300 μL serum-free DMEM were placed in the transwell chamber and 700 μL DMEM containing 20% FBS was added into the lower chamber. After incubated for about 24 h, the cells that migrated or invaded through the membrane were fixed with 4% paraformaldehyde and stained with crystal violet. Cells on the upper surface of the filter were removed by wiping with a small cotton swab. Images were captured of five randomly selected fields of the fixed cells, and the cells were counted using Image J software. All experiments were performed in triplicate.

For the cell migration and invasion assay in co-culture system, the mixed cells (the tumor cells were stably transfected with luciferase cDNA in advance) were resuspended in serum-free DMEM and then cultured in the upper chamber for 24 h. The cells that migrated or invaded through the membrane were isolated by trypsin digestion method and quantified by measuring luciferase activity using a Luciferase Assay System (Promega Corporation, USA).

ChIP analysis

About 5×10^6 cells were fixed in 1 % formaldehyde for 30 min at room temperature, and then DNA was sheared to an average fragment size of 500 to 1,000 bp by sonication. Subsequently, chromatin was immunoprecipitated with STAT3, p65, OCT1, ETS1, c-Myc and c-Jun antibodies, separately. A positive control antibody (RNA polymerase II/RPII), a negative control normal rabbit IgG, and GAPDH primers were used as controls to demonstrate the efficacy of the kit reagents (P-2025-48, Epigentek Group, USA). Purified chromatin was quantified by real-time PCR. Signals obtained from the ChIP assay were divided by signals obtained from an input sample. This input sample represented the amount of chromatin used in the ChIP assay. Here, 1 % of starting chromatin was used as the input, and then a dilution factor of 100 or 6.644 cycles (\log_2 of 100) was subtracted from the Ct value of diluted input. The primer pairs used for this analysis are described in supplementary Table S1.

Tumorigenicity assay in vivo

To evaluate the tumor promoting role of IL-6 *in vivo*, a HNC xenograft model was implemented in BALB/C nude mice (4-weeks-old). Briefly, CAL-27 cells were pretreated with or without 10 ng/mL rhIL-6 for 72 h. Then, a total of 1×10^6 CAL-27 cells in 100 μ L serum-free DMEM were subcutaneously injected into the left and right buttocks. The rhIL-6 group (n=5) was intraperitoneally injected with 100 ng rhIL-6 (in 100 μ L PBS) once a day, while the control group (n=5) was intraperitoneally injected with 100 μ L PBS. Eighteen days after transplantation,

xenografted tumors were collected and the tumor growth curve was plotted.

Experimental metastasis assay

Rca-T cell line was used to establish the HNC experimental metastasis model. Rca-T cells were pretreated with or without 10 ng/mL IL-6 for 72 h. Then, a total number of 1×10^6 Rca-T cells in 200 μ L serum-free DMEM were injected intravenously into the lateral tail vein of the 4-week-old athymic mice. The IL-6 group (n=5) was intraperitoneally injected with 100 ng IL-6 (in 100 μ L PBS) once a day, while the control group (n=5) was intraperitoneally injected with 100 μ L PBS. Two weeks later, the animals were sacrificed and the murine lungs were fixed in neutral-buffered formalin, embedded in paraffin, and cut into 4 μ m sections for further experiments.

Supplementary Figure legends

Figure S1. Overexpression of OPN in HNC tissues. (A) OPN gene expression in different cancer types including HNC according to the cBioPortal for Cancer Genomics. (B) OPN gene expression level in HNC according to the Cancer Genome Atlas (TCGA). Red indicates the up-regulated cases while the blue indicates the down-regulated cases.

Figure S2. Correlation between OPN mRNA level and clinicopathologic parameters. No significant associations were determined between OPN expression pattern and age (A), gender (B), alcohol history (C), pathological differentiation (D), local invasion (E), anatomic site (F) or tumor recurrence (G).

Figure S3. Identification of CAFs derived from HNC tissues. (A) Morphological images of NFs and CAFs under an inverted microscope and immunofluorescence stain for α -SMA and Vimentin of NFs and CAFs (Scale bar: 20 μ m). (B) Western blotting analyzed the expressions of α -SMA and Vimentin protein in 6 paired NFs and CAFs. (C) Patient-derived CAFs are KRAS wild type. CAFs (2 cases) were sequenced to determine if KRAS mutations were present in exon 2 at codon 12 and 13 (black outlined area). Both cells were identified as KRAS wild type.

Figure S4. NFs acquire the characteristics like CAFs after the interaction with

HNC cells. (A-C) The luciferase-expressing CAL-27 and SCC-25 cells were co-cultured with NFs or CAFs, and their proliferative, migratory and invasive abilities were analyzed. CAFs significantly promoted HNC cell proliferation, migration and invasion than NFs did. (D) The protein levels of Vimentin and α -SMA were determined in NFs after co-culture with HNC cells. (E-G) CAL-27 and SCC-25 cells were incubated with NFs CM or the CM of NFs after co-culture with HNC cells (C-NFs CM) for 72 h, and the proliferative, migratory and invasive abilities of CAL-27 and SCC-25 cells were determined using cell proliferation assay, transwell migration and invasion assay (Scale bar: 100 μ m). (* p <0.05; ** p <0.01; *** p <0.001; **** p <0.0001)

Figure S5. Functional analyses of the effects of OPN on HNC cell proliferation, migration and invasion. (A, B) Recombinant human OPN promoted the proliferation of SCC-25 cells in a dose-dependent manner, while neutralization of OPN with OPN antibody (5 μ g/mL) inhibited the proliferation of HN6 cells. (C, D) Recombinant human OPN (0.5 μ M) triggered the migration and invasion of SCC-25 cells, while OPN neutralizing antibody (5 μ g/mL) inhibited the migration and invasion of HN6 cells. (E, F) Overexpression of OPN in SCC-25 cells facilitated the proliferation of tumor cells, while OPN knockdown in HN6 cells significantly inhibited the proliferative ability of tumor cells. (G-I) Overexpression of OPN in SCC-25 cells facilitated the migration, invasion, and plate and soft agar colony formation of tumor cells. (J-L) OPN knockdown with specific siRNA in HN6 cells significantly inhibited

the migration, invasion and colony formation of tumor cells. (Scale bar, migration: 100 μm ; invasion: 100 μm ; plate colony formation: 5 mm; soft agar colony formation: 100 μm) (ns, no significant difference; * p <0.05; ** p <0.01; *** p <0.001; **** p <0.0001)

Figure S6. OPN expression in HNC cells after OPN knockdown or overexpression. (A, B) The results of western blotting and real-time PCR showing OPN expression levels in CAL-27 and SCC-25 cells after transfection of OPN expression vector, and an increased supernatant OPN level was observed. (C, D) The results of western blotting and real-time PCR showing OPN expression levels in HN4 and HN6 cells after transfection of specific siRNAs targeting OPN, and a decreased supernatant OPN level was detected. (** p <0.01; *** p <0.001; **** p <0.0001)

Figure S7. Functional analyses of the effects of OPN on HNC cell migration. (A, B) The wound healing assay revealed that overexpression of OPN in CAL-27 and SCC-25 cells promoted the migratory activity of tumor cells (Scale bar: 100 μm). (C, D) OPN knockdown in HN4 and HN6 cells inhibited the migration of tumor cells (Scale bar: 100 μm). (* p <0.05; ** p <0.01)

Figure S8. Stromal IL-6 induces the expression of neoplastic OPN during the interactions between HNC cells and fibroblasts. (A, B) The mRNA levels of TGF- β 1, TGF- β 2, TGF- β 3, IL-1A, IL-6, TNF α , PDGFA, PDGFB, FGF2 and EGF in

HNC cells (A) and NFs (B) were detected after the co-culture of NFs and HN4 cells by real-time PCR. (C, D) IL-6 induced OPN expression in SCC-25 cells in a dose-dependent and time-dependent manner. Protein expression by western blot analysis and mRNA expression by real-time PCR were measured at the indicated concentrations. (E, F) OPN overexpression in SCC-25 cells or OPN knockdown in HN6 cells showed little influence on IL-6 expression at the mRNA level. (G) The protein and mRNA levels of neoplastic OPN in SCC-25 cells were increased after co-culture with NFs and antagonized by IL-6-neutralizing antibody (5 $\mu\text{g}/\text{mL}$). (H) The model presents a method to detect the proliferation, migration and invasion of HNC cells involved in a co-culture system. (I-K) Both OPN (5 $\mu\text{g}/\text{mL}$) and IL-6 (5 $\mu\text{g}/\text{mL}$) neutralizing antibodies partially inhibited the NF-mediated proliferation, migration and invasion of SCC-25 cells, and the combination of OPN and IL-6 antibodies was superior to each of them alone. (ns, no significant difference; * $p < 0.05$; ** $p < 0.01$; *** $p < 0.001$; **** $p < 0.0001$)

Figure S9. Correlation analysis between OPN expression and TGF- β s. TGF- β 1 (A), TGF- β 2 (B) and TGF- β 3 (C) mRNA levels were determined using real-time PCR in 80 HNC tissues and in 96 normal oral epithelial tissues. No significant correlation was observed between the TGF- β s and OPN expression levels in the HNC tissues (n=80).

Figure S10. IL-6 is highly expressed in HNC-derived CAFs. (A)

Immunohistochemical analysis of IL-6 protein expression in HNC tissues and matched adjacent normal tissues, and the IL-6 expression mainly enriched in the tumor stroma (Scale bar, 200×: 50 μm; 400×: 25 μm). (B) Higher IL-6 staining was observed in HNC tissue compared to adjacent normal tissues. MOD, mean optical density. (C) IL-6 protein expression level in HNC tissue and matched normal tissues was quantified by ELISA after being grinded into tissue homogenate. (D) IL-6 mRNA expression level in NFs, CAFs and tumor cells was detected by real-time PCR. (E) IL-6 protein expression level in the CM of NFs, CAFs and tumor cells was measured by ELISA. (* $p < 0.05$; ** $p < 0.01$; *** $p < 0.001$)

Figure S11. STAT3 binding to OPN promoter is required for IL-6-induced OPN expression. (A) Diagram showing the OPN 5' flanking DNA. A 2,000 bp OPN promoter segment was divided into 4 compartments and primers were designed respectively for each compartment. (B) CAL-27 cells were incubated with or without IL-6 (10 ng/mL) for 3 h in advance. ChIP assays using anti-STAT3, anti-p65, anti-c-Myc, anti-OCT1, anti-ETS1, anti-c-Jun or anti-IgG antibodies were performed to determine the affinity of these transcription factors for the OPN promoter in CAL-27 cells. (C) CAL-27 cells were pre-treated with 5 μM Cryptotanshinone (a STAT3 inhibitor purchased from Selleck) for 2 h followed by treatment with 10 ng/mL IL-6 for 48 h. The protein levels of STAT3, p-STAT3 (Tyr705) and OPN were detected by western blotting, and the mRNA level of OPN was measured using real-time PCR. (D) CAL-27 cells were transiently transfected with STAT3 specific

siRNAs for 24 h followed by treatment with or without 10 ng/mL IL-6 for 48 h. The protein levels of STAT3, p-STAT3 (Tyr705) and OPN were detected by western blotting, and the mRNA level of OPN was measured using real-time PCR. (ns, no significant difference; * $p < 0.05$; ** $p < 0.01$; *** $p < 0.001$)

Figure S12. IL-6 promotes the proliferation, migration and invasion of HNC cells *in vitro* and tumor metastasis *in vivo*. (A) Recombinant human IL-6 (10 ng/mL) promoted the proliferation of CAL-27 and SCC-25 cells. (B) IL-6 neutralizing antibody (5 μ g/mL) inhibited the growth of CAL-27 and SCC-25 cells. (C, D) Recombinant human IL-6 (10 ng/mL) triggered the migration and invasion of CAL-27 and SCC-25 cells, while IL-6 neutralizing antibody (5 μ g/mL) inhibited the migration and invasion of CAL-27 and SCC-25 cells (Scale bar: 100 μ m). (E) IL-6 treatment (intraperitoneally injected with 100 ng IL-6 once a day per mouse) facilitated the xenograft tumor growth in nude mice. (F) IL-6 treatment (intraperitoneally injected with 100 ng IL-6 once a day per mouse) promoted the formation and growth of metastatic nodules in nude mice (Scale bar, left: 5 mm; right: 50 μ m). (* $p < 0.05$; ** $p < 0.01$; *** $p < 0.001$)

Figure S13. CAF-derived IL-6 promotes the proliferation, migration and invasion of HNC cells by modulating the OPN expression. (A) The protein level and mRNA level of OPN were determined in CAL-27 and SCC-25 cells after co-culture with CAFs. (B) The protein and mRNA levels of neoplastic OPN in

CAL-27 and SCC-25 cells were increased after co-culture with CAFs and antagonized by IL-6-neutralizing antibody (5 µg/mL). (C) Both OPN (5 µg/mL) and IL-6 (5 µg/mL) neutralizing antibodies partially inhibited the CAF-mediated proliferation, migration and invasion of CAL-27 cells, and the combination of OPN and IL-6 antibodies was superior to each of them alone. (* $p < 0.05$; ** $p < 0.01$; *** $p < 0.001$)

Figure S14. Contribution of NF- or CAF-derived IL-6 in HNC cell proliferation, migration and invasion. (A) The protein level of IL-6 was determined in 4 paired NFs and CAFs using western blotting. (B-D) The results of western blotting and real-time PCR showing IL-6 expression levels in NFs and CAFs after transfection of specific shRNAs targeting IL-6, and a decreased supernatant IL-6 level was detected. (E) The NF- or CAF-mediated proliferation, migration and invasion of SCC-25 cells were partly decreased when the fibroblasts were transfected with shRNA targeting IL-6 in advance. (* $p < 0.05$; ** $p < 0.01$; *** $p < 0.001$)

Figure S15. OPN promotes the proliferation, migration and invasion of HNC cells through the integrin $\alpha\beta3$ -NF-kappa B axis. (A, B) SCC-25 cells were treated with 0.5 µM rhOPN for 3 h or pre-treated with 100 µM PDTC or 20 µg/mL integrin $\alpha\beta3$ antibody for 1 h followed by treatment with 0.5 µM rhOPN for 3 h. Immunofluorescence assays and western blot analysis were used to assess the location of p65 in SCC-25 cells (Scale bar: 20 µm). (C, D) Western blot analysis of I κ B α degradation, phosphorylated I κ B α (Ser 32/36), p65 and phosphorylated p65 (Ser 468

and Ser 536) in SCC-25 cells following treatment with rhOPN or OPN overexpression. (E) Constitutive NF-kappa B-response promoter activity. Recombinant human OPN, as well as OPN-enriched CM stimulated the NF-kappa B transcriptional activity, and pretreatment with PDTC partly inhibited this effect. LPS (50 ng/mL) was used as a positive control. (F) OPN overexpression in SCC-25 cells stimulated the mRNA expression of MMP2, MMP9, uPA and ICAM-1. (G) Recombinant human OPN directly induced the expression of MMP2, MMP9, uPA and ICAM-1 in SCC-25 cells, and the expression was partially suppressed when pre-treated with PDTC. (H) The OPN-induced SCC-25 cell growth, migration and invasion were partly neutralized by pretreatment with PDTC. (ns, no significant difference; * p <0.05; ** p <0.01; *** p <0.001; **** p <0.0001)

Figure S16. OPN induced the NF-kappa B transcriptional activity in HNC. (A, B)

Immunohistochemical analysis of OPN, nuclear p65, MMP2, MMP9, uPA and ICAM-1 expressions in CAL-27, CAL-27-OPN, CAL-27+NFs and CAL-27+NFs+OPN antibody xenografted tumors. MOD, mean optical density (Scale bar, 200×: 50 μ m; 400×: 25 μ m). (ns, no significant difference; * p <0.05; ** p <0.01; *** p <0.001; **** p <0.0001)

Figure S17. Prognostic and diagnostic significance of OPN and IL-6 for HNC

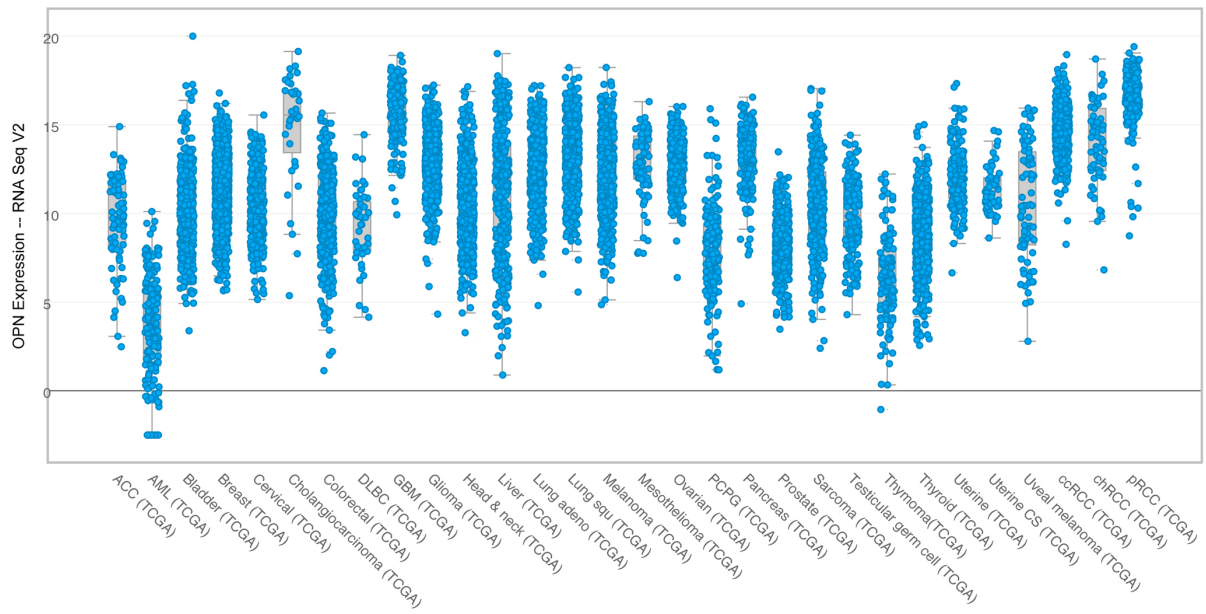
patients. (A) Kaplan-Meier analyses of the overall survival. Patients with high IL-6 expression were associated with a significantly lower overall survival rate than

patients with low IL-6 expression ($p=0.004$). (B) IL-6 plasma concentration (pg/mL) in HNC patients and healthy controls. (C) Positive correlation between plasma OPN level and plasma IL-6 level. (D-F) Receiver operating characteristic (ROC) curve analysis of the OPN and IL-6 mRNA stratified by different groups in the validation set. ROC plots for the OPN and IL-6 mRNA discriminating the five-year survival group from the death group (D), the TNM stage I group from the healthy group (E) and the metastasis group from the non-metastasis group (F). AUC, area under the curve. (G, H) ROC curve analysis of the plasma OPN and IL-6 stratified by different groups in the validation set. ROC plots for the plasma OPN, IL-6 as well as the panel of plasma OPN and IL-6 discriminating the TNM stage I group from the healthy group (G) and the metastasis group from the non-metastasis group (H).

Supplementary Table legends

Table S1. The primers used for real-time PCR

A



B

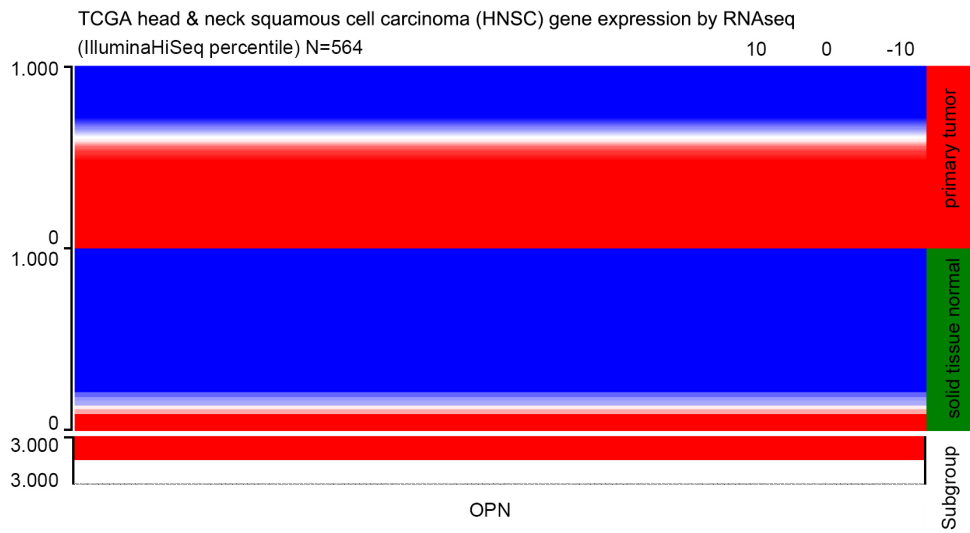


Figure S1

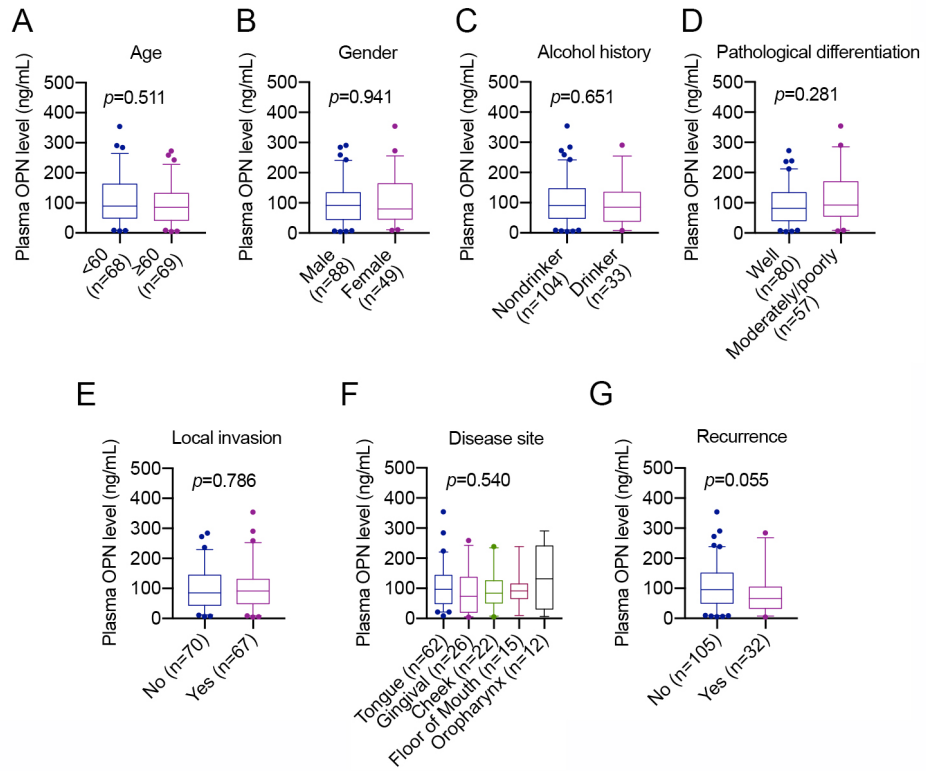


Figure S2

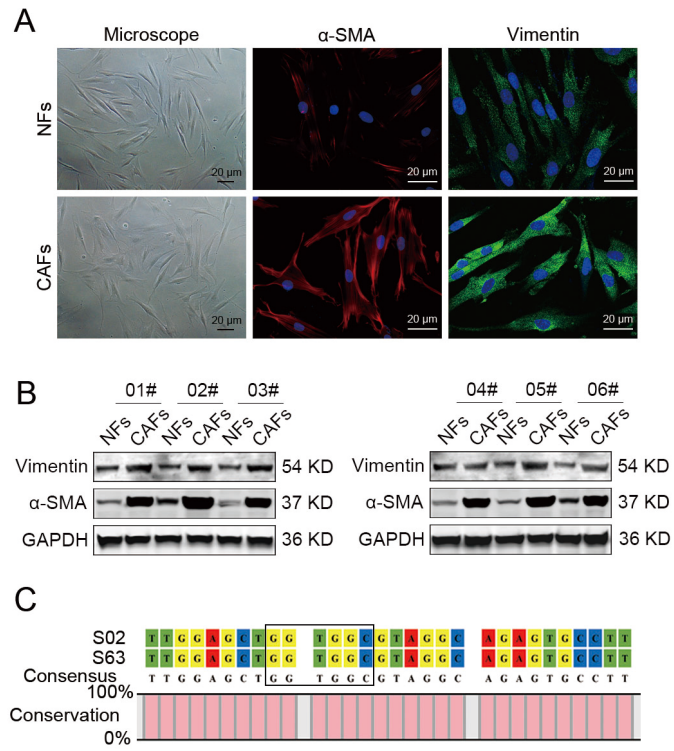


Figure S3

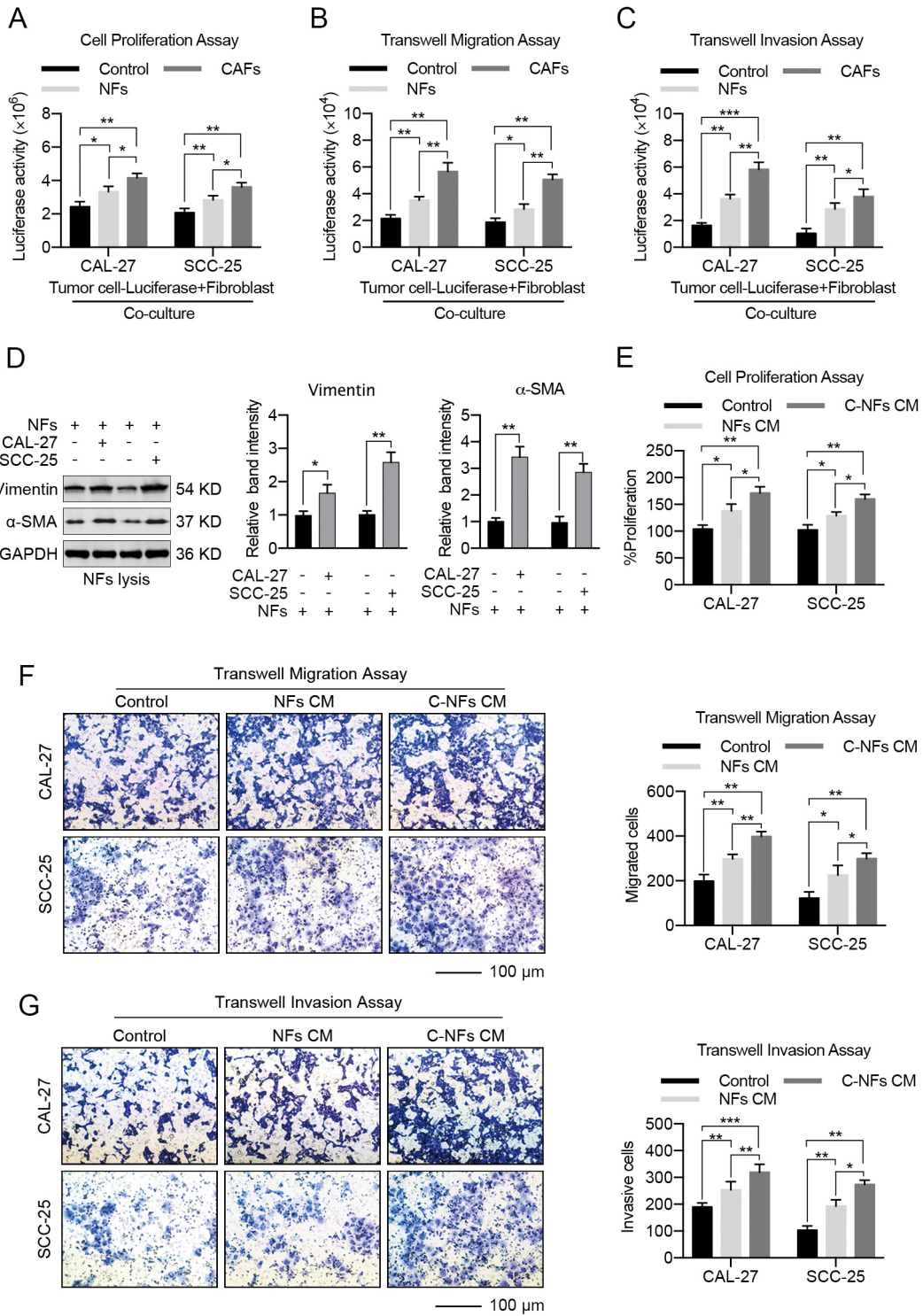


Figure S4

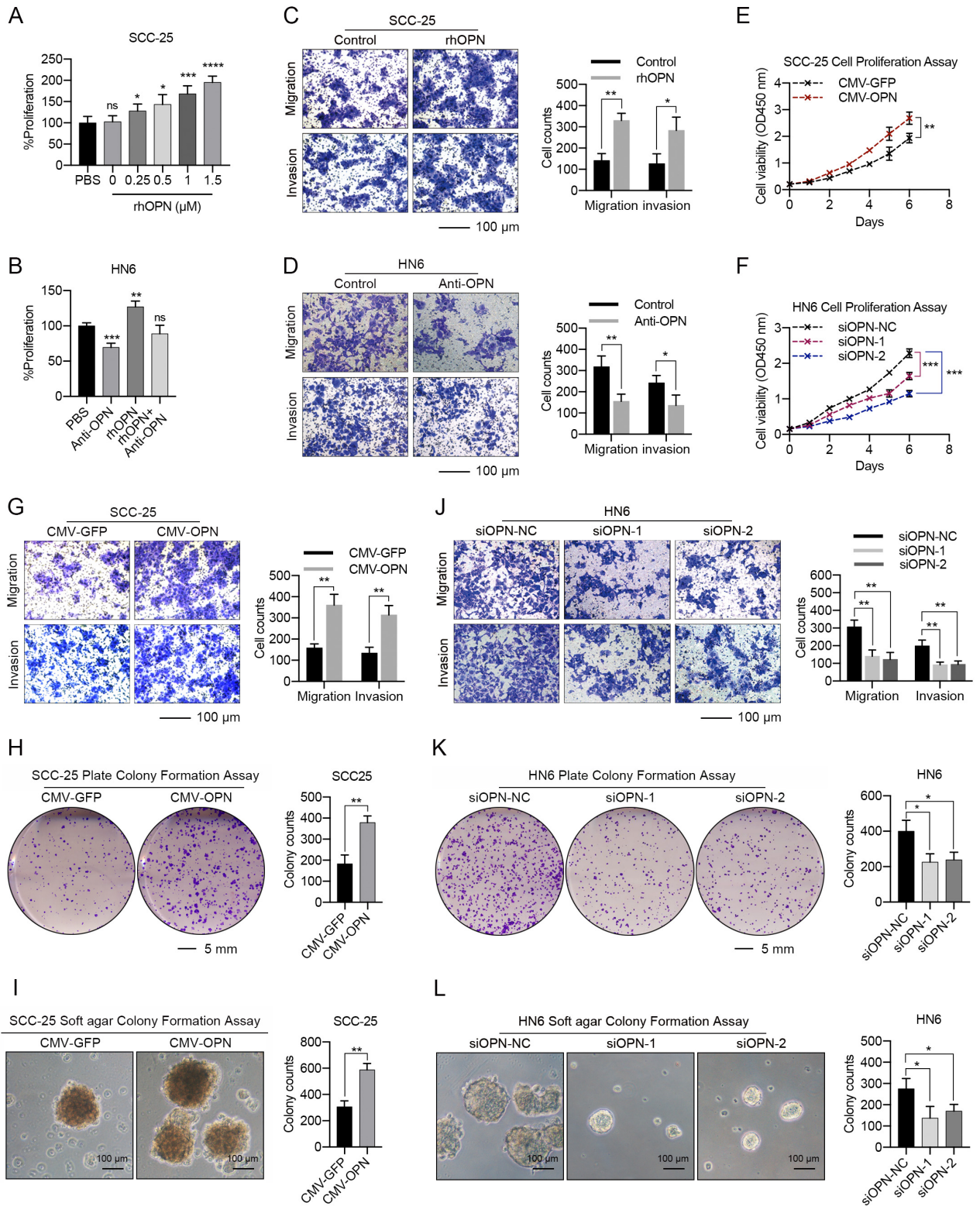


Figure S5

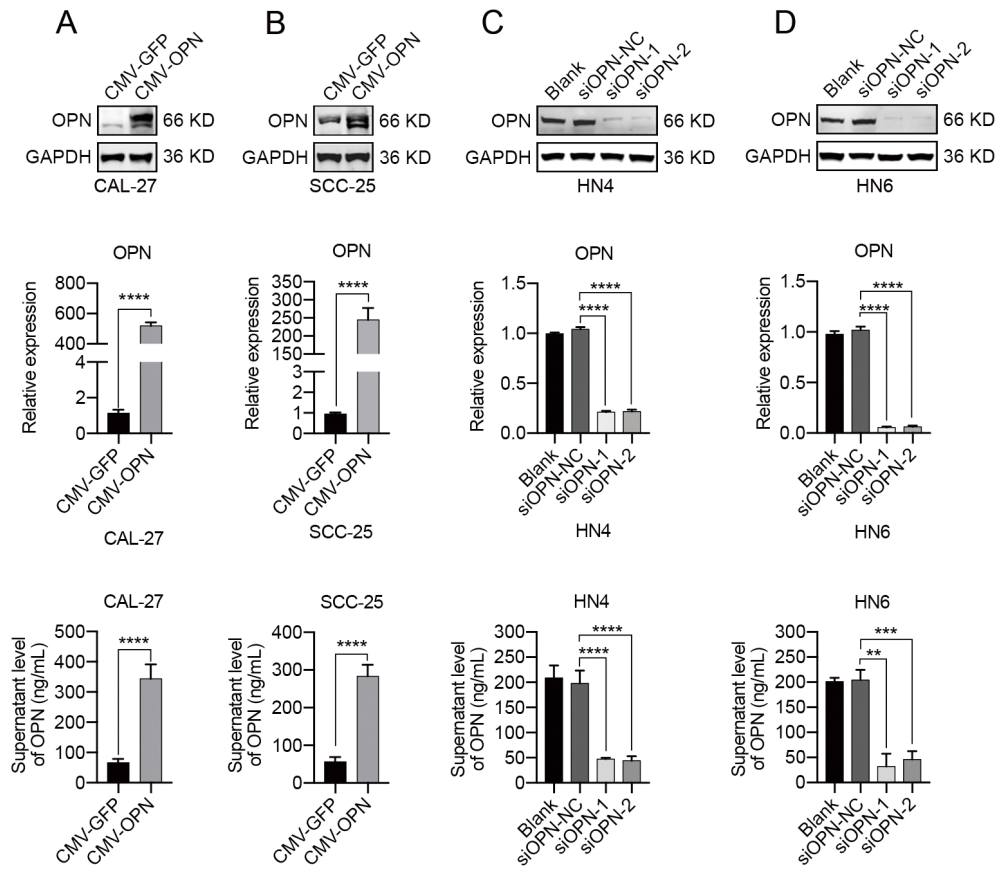


Figure S6

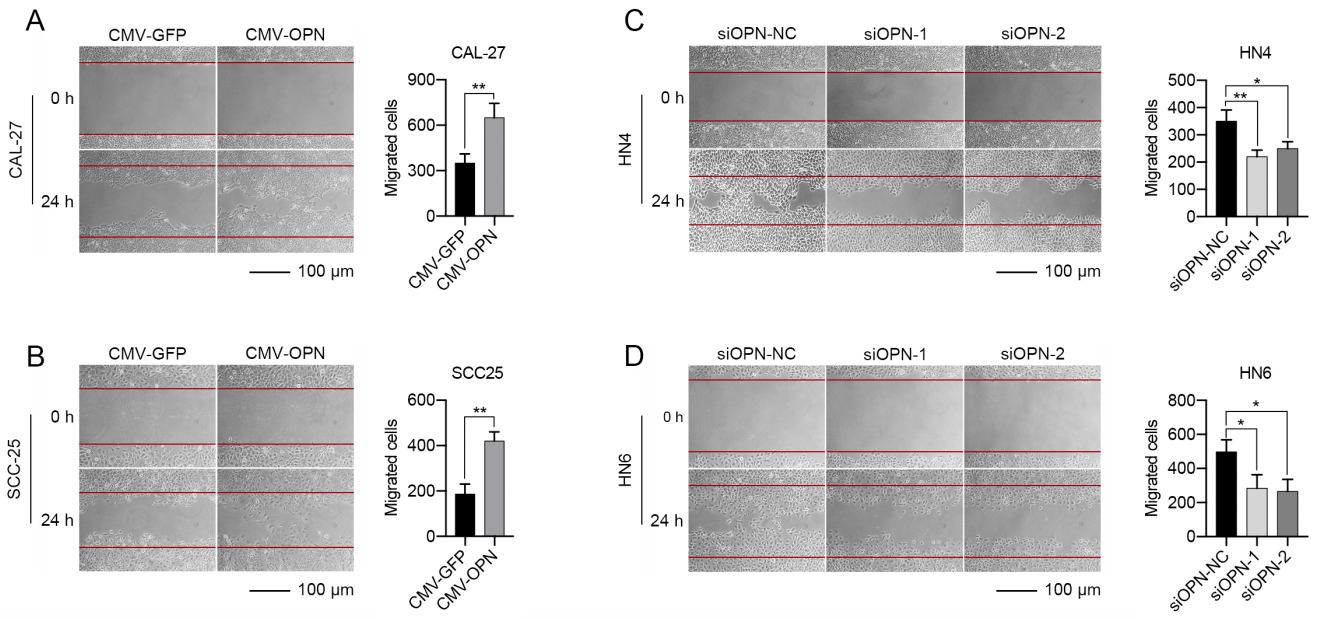


Figure S7

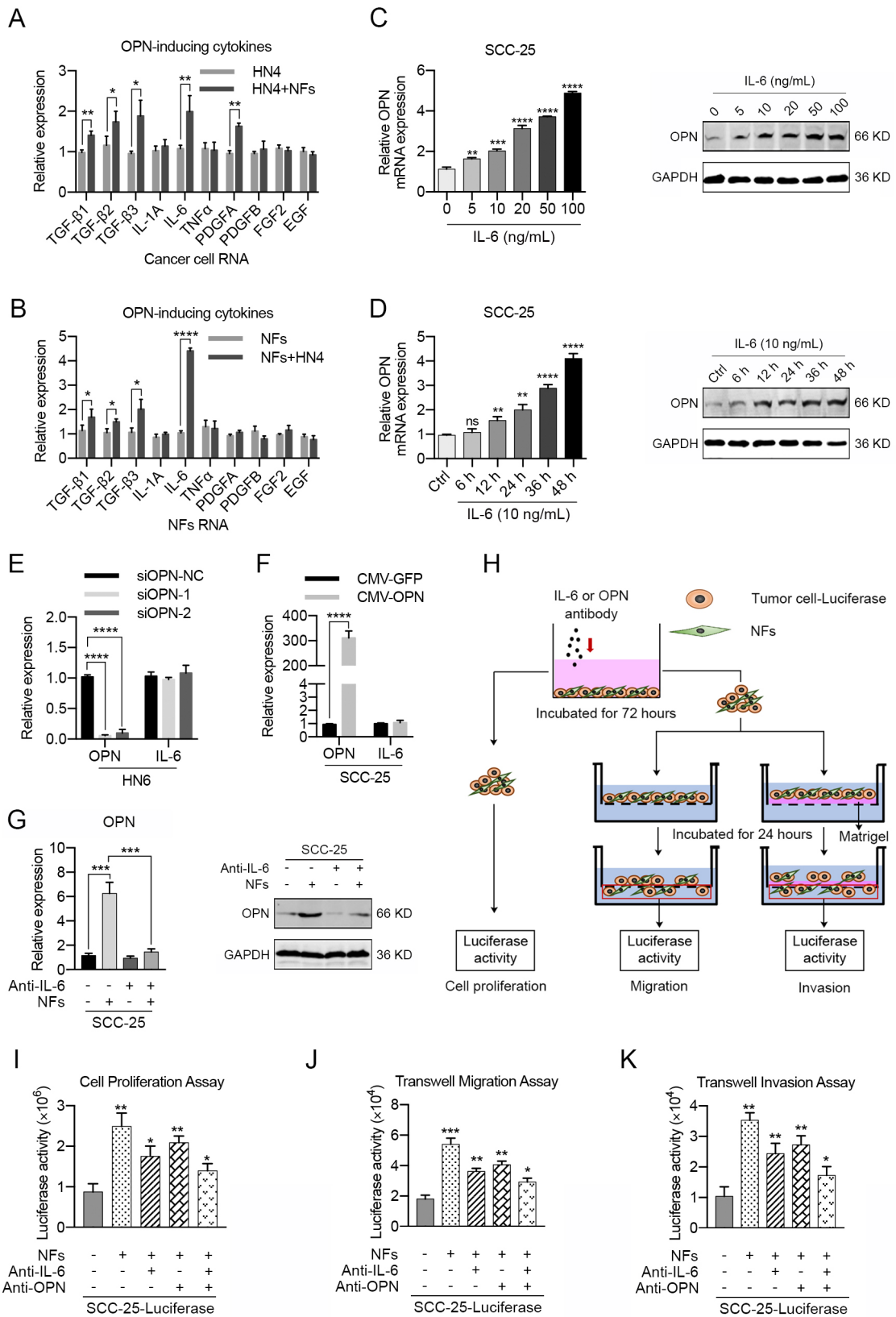


Figure S8

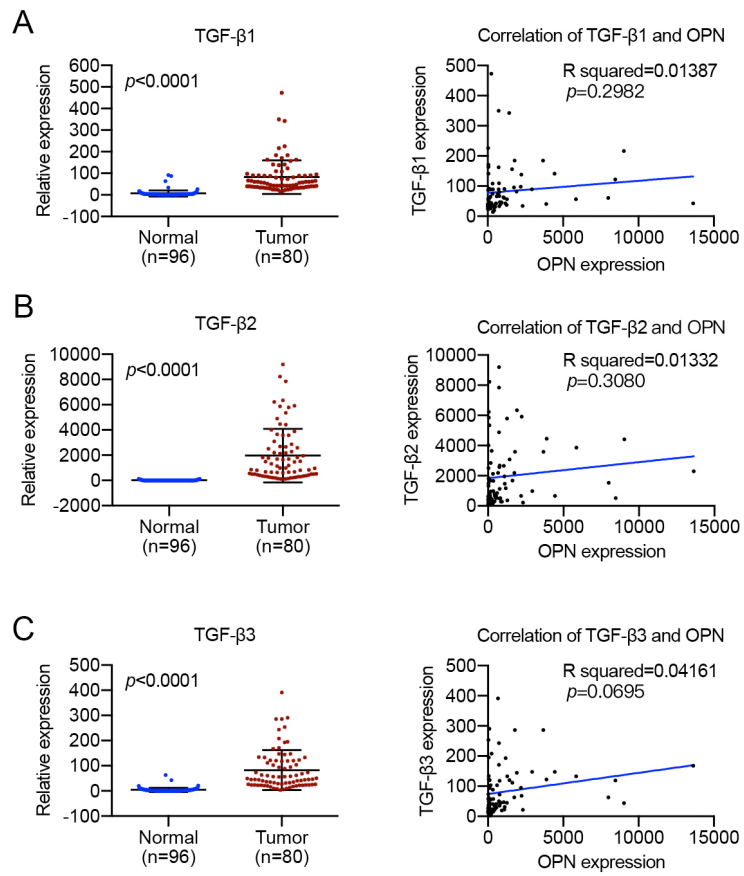


Figure S9

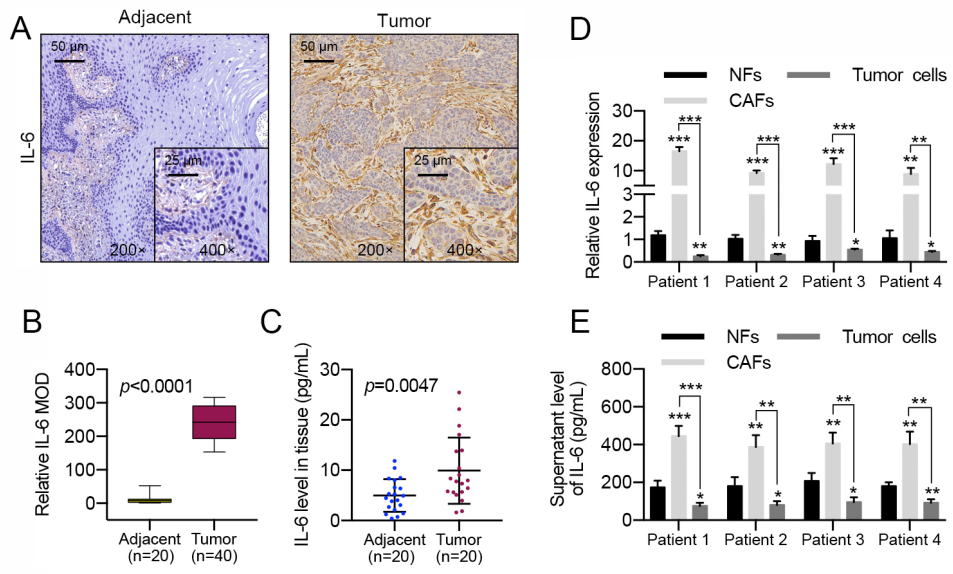


Figure S10

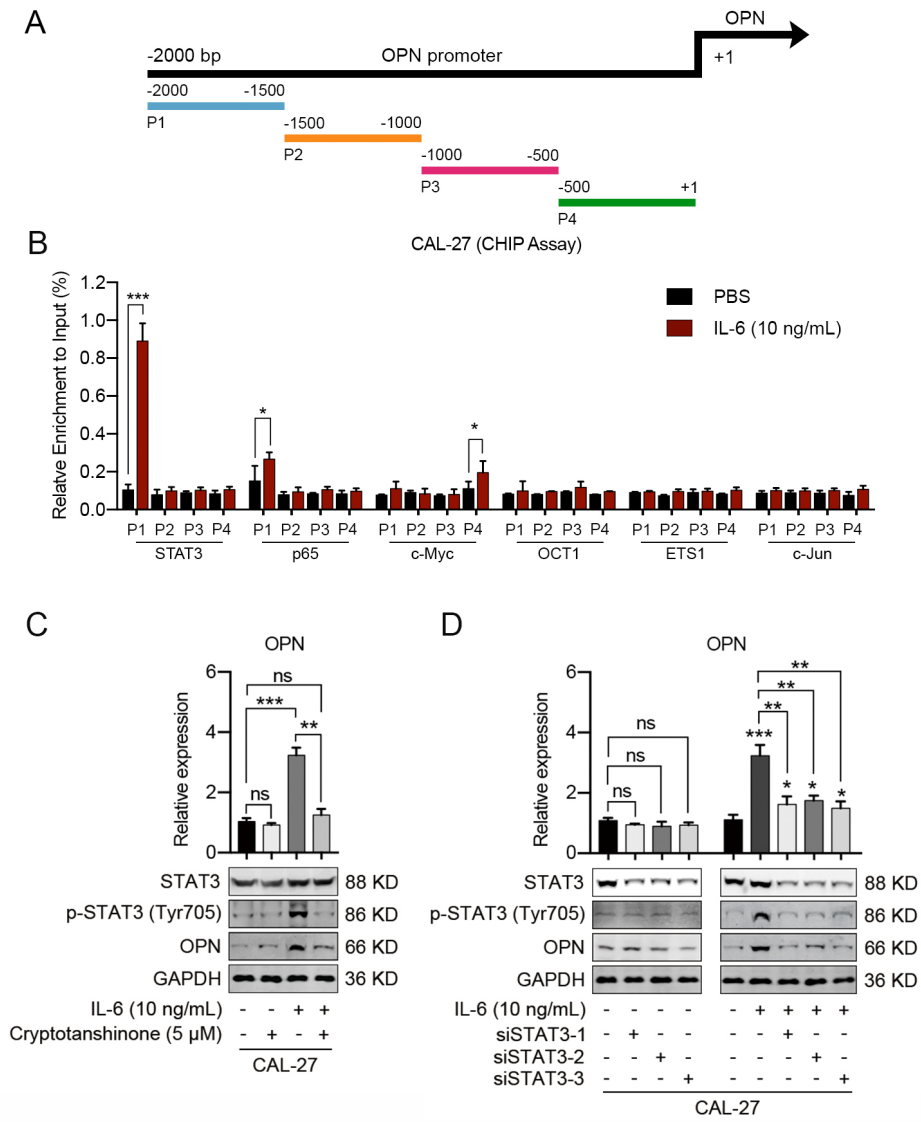


Figure S11

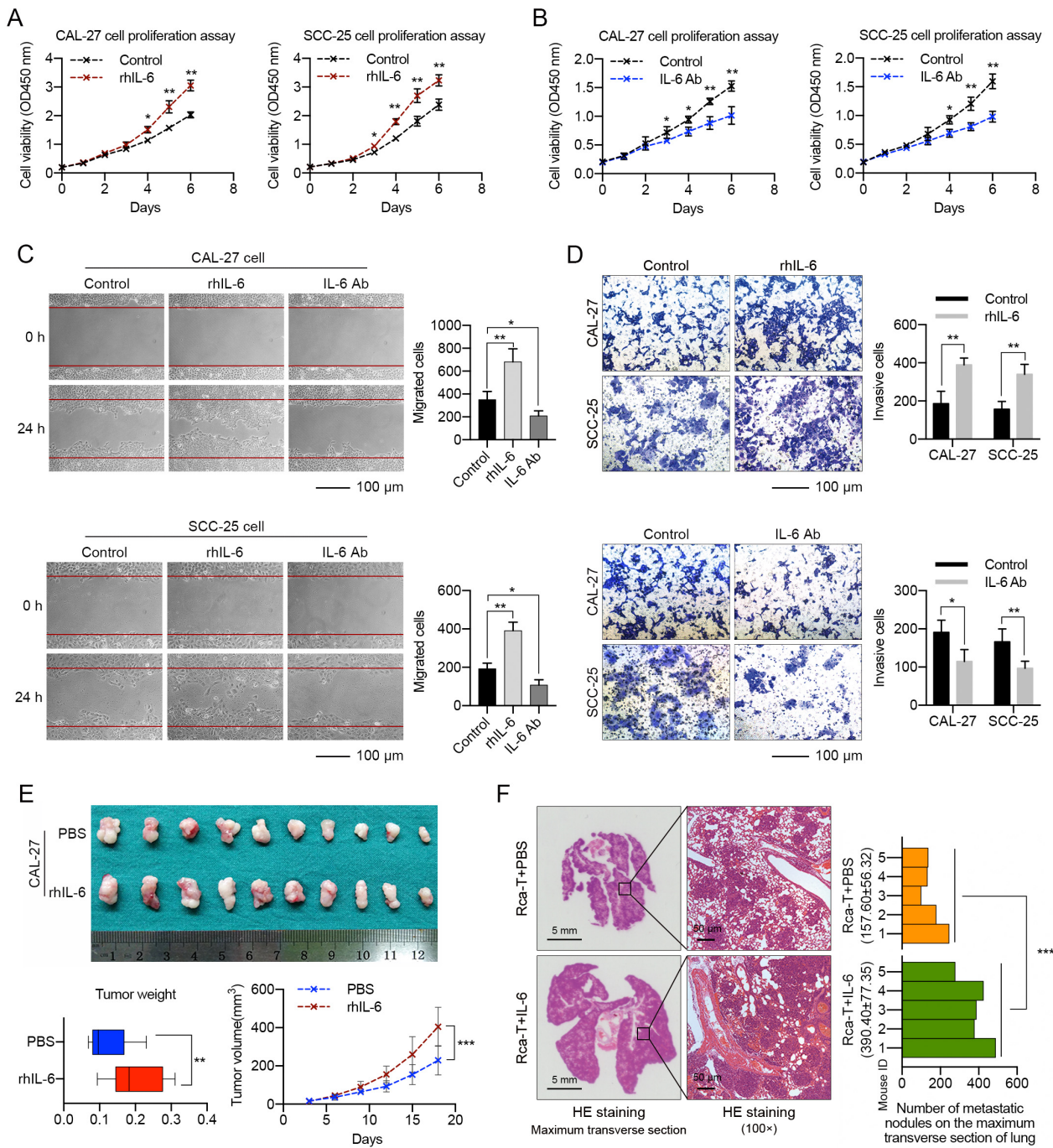


Figure S12

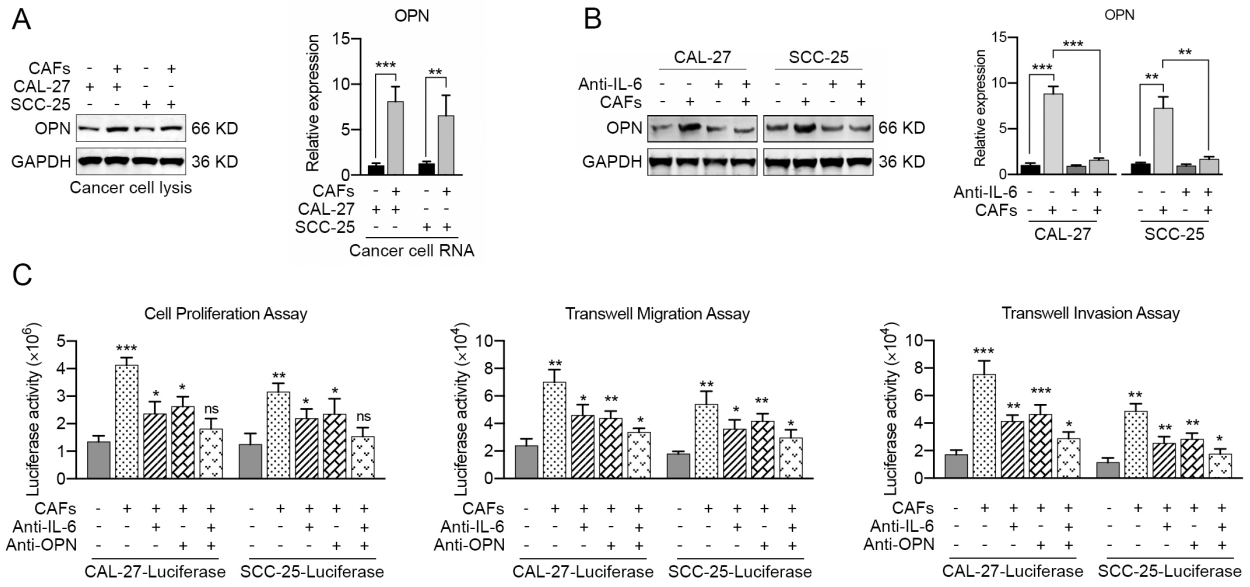


Figure S13

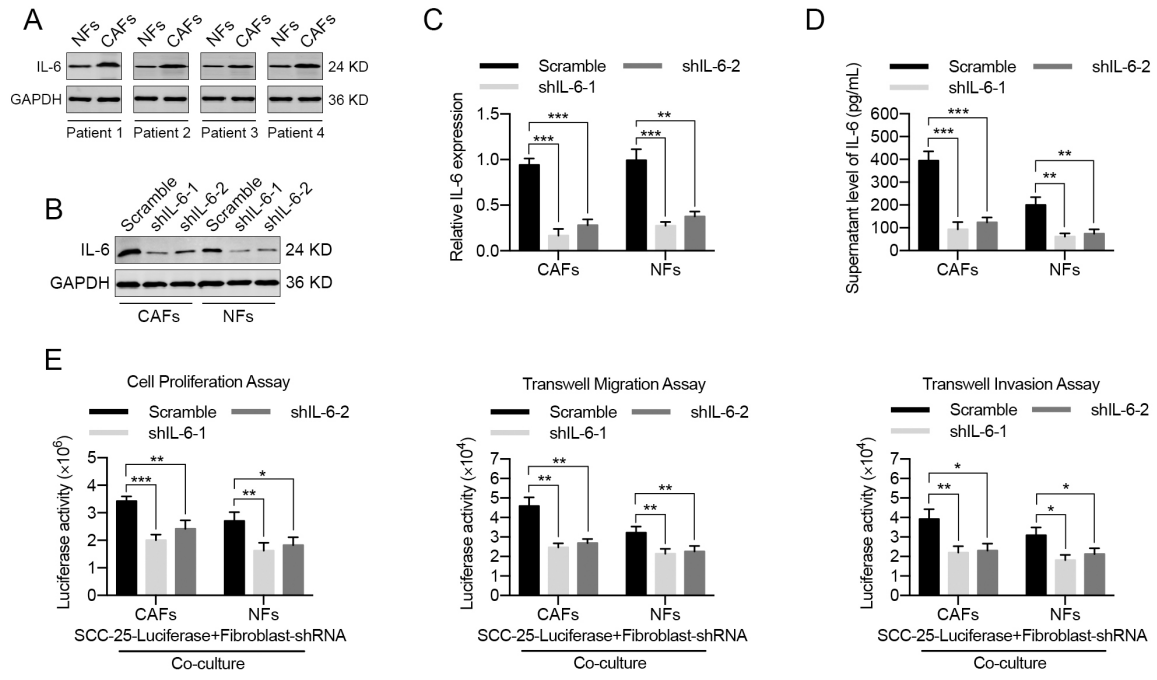


Figure S14

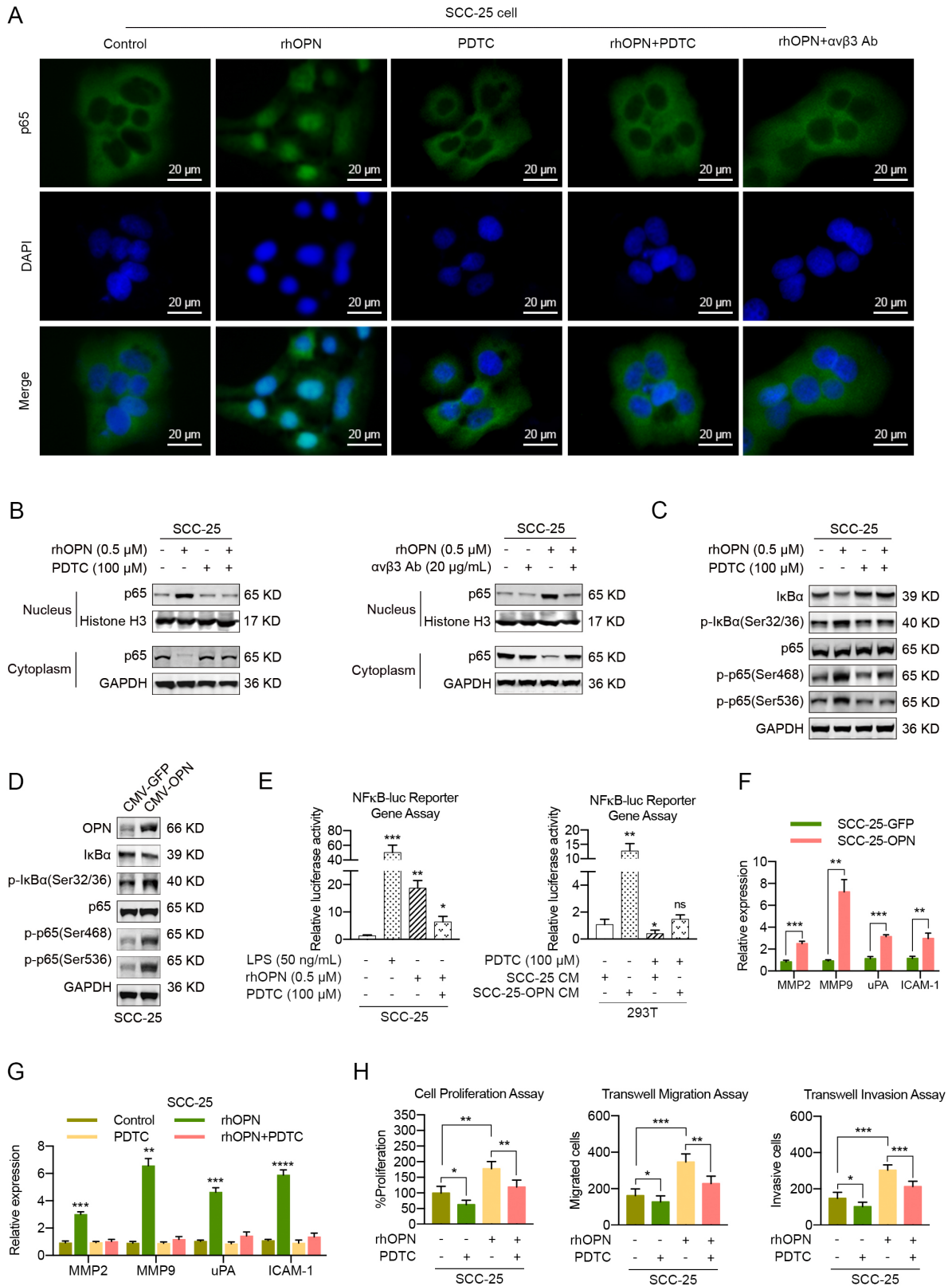
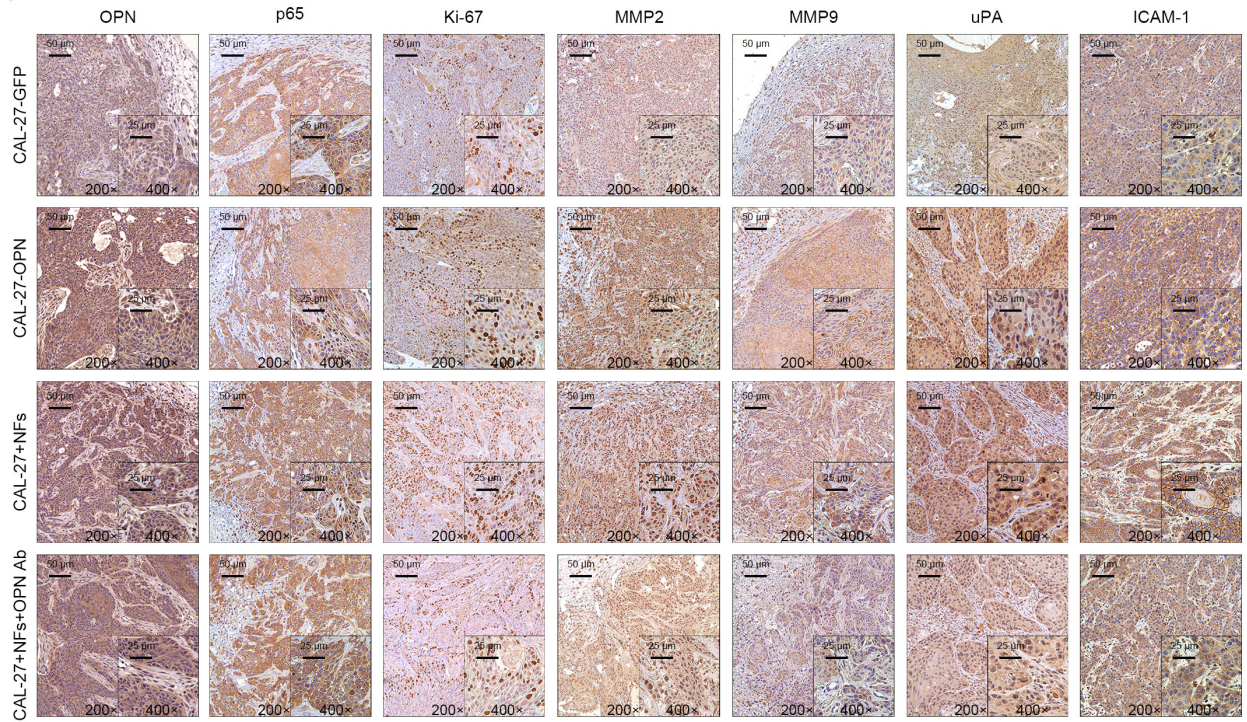


Figure S15

A



B

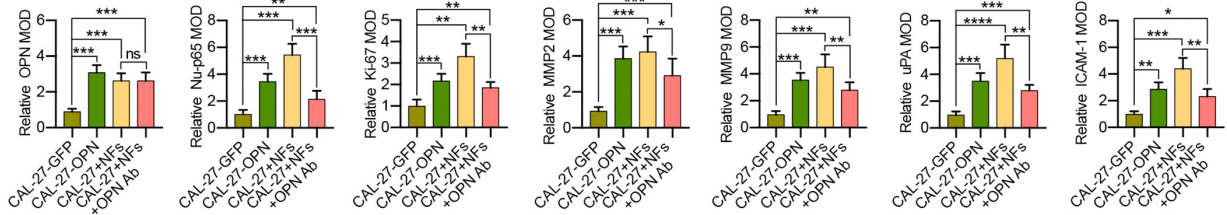


Figure S16

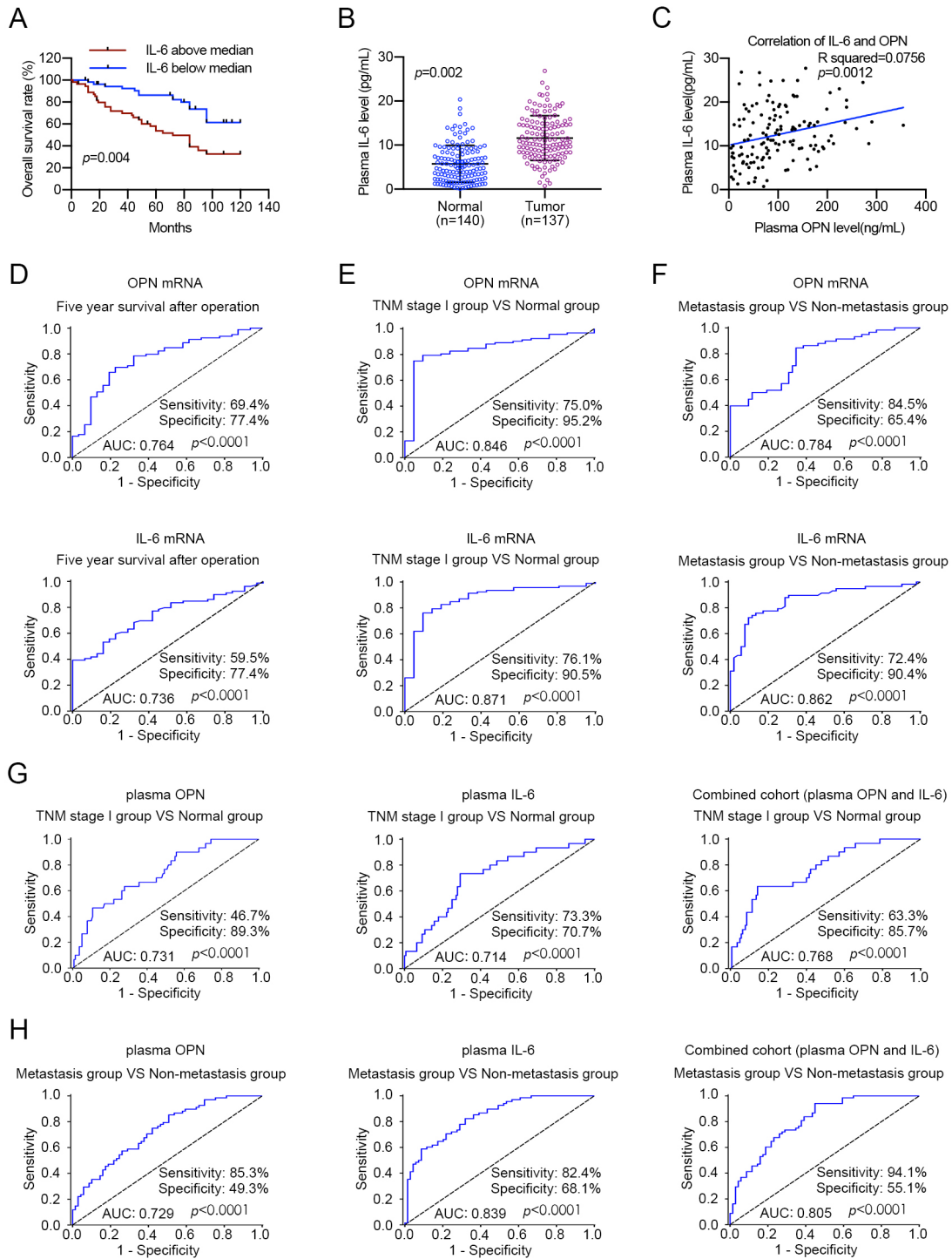


Figure S17

Table S1. The primers used for real-time PCR

| Genes | Primer sequences |
|---------------------|--|
| Human <i>OPN</i> | forward 5'-GAAGTTTCGCAGACCTGACAT-3' |
| | reverse 5'-GTATGCACCATTCAACTCCTCG-3' |
| Human <i>TGF-β1</i> | forward 5'-TCGCCAGAGTGGTTATCTTTTG-3' |
| | reverse 5'-AGGAGCAGTGGGCGCTAAG-3' |
| Human <i>TGF-β2</i> | forward 5'-ATCCCGCCCACTTTCTAC-3' |
| | reverse 5'-GCTCAATCCGTTGTTTCAGG-3' |
| Human <i>TGF-β3</i> | forward 5'-GCCCTTGCCCATACCTCCGC-3' |
| | reverse 5'-CGCAGCAAGGCGAGGCAGAT-3' |
| Human <i>IL1A</i> | forward 5'-AGATGCCTGAGATACCCAAAACC-3' |
| | reverse 5'-CCAAGCACACCCAGTAGTCT-3' |
| Human <i>IL-6</i> | forward 5'-ACTCACCTCTTCAGAACGAATTG-3' |
| | reverse 5'-CCATCTTTGGAAGGTTTCAGGTTG-3' |
| Human <i>TNFα</i> | forward 5'-GAGGCCAAGCCCTGGTATG-3' |
| | reverse 5'-CGGGCCGATTGATCTCAGC-3' |
| Human <i>PDGFA</i> | forward 5'-GCAAGACCAGGACGGTCATTT-3' |
| | reverse 5'-GGCACTTGACACTGCTCGT-3' |
| Human <i>PDGFB</i> | forward 5'-CTCGATCCGCTCCTTTGATGA-3' |
| | reverse 5'-CGTTGGTGCGGTCTATGAG-3' |
| Human <i>FGF2</i> | forward 5'-AGAAGAGCGACCCTCACATCA-3' |
| | reverse 5'-CGGTTAGCACACACTCCTTTG-3' |
| Human <i>EGF</i> | forward 5'-TGTCCACGCAATGTGTCTGAA-3' |
| | reverse 5'-CATTATCGGGTGAGGAACAACC-3' |
| Human <i>MMP2</i> | forward 5'-TACAGGATCATTGGCTACACACC-3' |
| | reverse 5'-GGTCACATCGCTCCAGACT-3' |
| Human <i>MMP9</i> | forward 5'-TGTACCGCTATGGTTACTCTCG-3' |
| | reverse 5'-GGCAGGGACAGTTGCTTCT-3' |
| Human <i>uPA</i> | forward 5'-GGGAATGGTCACTTTTACCGAG-3' |
| | reverse 5'-GGGCATGGTACGTTTGCTG-3' |
| Human <i>ICAM-1</i> | forward 5'-ATGCCAGACATCTGTGTCC-3' |
| | reverse 5'-GGGGTCTCTATGCCCAACAA-3' |

| | |
|---------------------------------------|---|
| Human <i>β-actin</i> | forward 5'-TCACCCACACTGTGCCCATCTACGA-3' |
| | reverse 5'-CAGCGGAACCGCTCATTGCCAATGG-3' |
| Human <i>OPN-P1</i> | forward 5'-TATCCCGCTGGAATTAAGAA-3' |
| | reverse 5'-GAGATGAACCATACGACCCT-3' |
| Human <i>OPN-P2</i> | forward 5'-GAGAAAGCAAATGAAGAT-3' |
| | reverse 5'-AAAATTACAGGGAAAGTC-3' |
| Human <i>OPN-P3</i> | forward 5'-TGAGGGAACAAGGATAGG-3' |
| | reverse 5'-TGCTTCAGGAGCCAGACC-3' |
| Human <i>OPN-P4</i> | forward 5'-TCATACAGGCAAGAGTGGT-3' |
| | reverse 5'-AAGGGAGAAAGTAGGGAAA-3' |
| Human <i>GAPDH</i> | forward 5'-TACTAGCGGTTTTACGGGCG-3' |
| | reverse 5'-TCGAACAGGAGGAGCAGAGAGCGA-3' |